Please cite this article in press as: Hsiao et al., Synthesis of a Phosphoantigen Prodrug that Potently Activates Vγ9Vδ2 T-Lymphocytes, Chemistry & Biology (2014), http://dx.doi.org/10.1016/j.chembiol.2014.06.006

Chemistry & Biology
Article

Synthesis of a Phosphoantigen Prodrug that Potently Activates Vγ9Vδ2 T-Lymphocytes

Chia-Hung Christine Hsiao,[1] Xiaochen Lin,[1] Rocky J. Barney,[2,3] Rebekah R. Shippy,[2] Jin Li,[1] Olga Vinogradova,[1] David F. Wiemer,[2,4] and Andrew J. Wiemer[1,*]
[1]Department of Pharmaceutical Sciences, University of Connecticut, Storrs, CT 06269, USA
[2]Department of Chemistry, University of Iowa, Iowa City, IA 52242, USA
[3]Department of Chemistry, Western Wyoming Community College, Rock Springs, WY 82901, USA
[4]Department of Pharmacology, University of Iowa, Iowa City, IA 52242, USA
*Correspondence: andrew.wiemer@uconn.edu
http://dx.doi.org/10.1016/j.chembiol.2014.06.006

SUMMARY

Phosphoantigen-sensitive Vγ9Vδ2 T cells are important responders to infections and malignancy. However, the mechanisms by which phosphoantigens stimulate Vγ9Vδ2 T cells are unclear. Here, we synthesized phosphoantigen prodrugs and used them to demonstrate that intracellular delivery of phosphoantigens is required for their activity. The pivaloyloxymethyl prodrug is the most potent phosphoantigen described to date, with stronger stimulation of Vγ9Vδ2 T cells from human peripheral blood and greater ability to induce lysis of Daudi lymphoma cells relative to the previously most potent compound, (E)-4-hydroxy-3-methyl-but-2-enyl pyrophosphate (HMBPP). We demonstrate high binding affinity between phosphoantigens and the intracellular region of butyrophilin 3A1 (BTN3A1), localized to the PRY/SPRY (B30.2) domain, but also affecting the membrane proximal region. Our findings promote a phosphoantigen prodrug approach for cancer immunotherapy and unravel fundamental aspects of the mechanisms of Vγ9Vδ2 T cell activation.

INTRODUCTION

The cells of the immune system recognize diverse foreign- and self-antigens, generating responses that remove a variety of foreign invaders with great specificity. As such, generation of drug-like molecules that can regulate immune cell function is of wide interest. The γδ T cells, usually only comprising 1%–10% of circulating T cells, have received attention recently due to their function in cancer immunosurveillance (Bonneville et al., 2010). Unlike the αβ T cells that respond to peptides, a subset of γδ T cells (Vγ9Vδ2 T cells) detects small phosphorous-containing compounds (phosphoantigens) (Wiemer and Wiemer, 2014). The Vγ9Vδ2 T cells most likely gained sensitivity to phosphoantigens to fight bacterial infections, given that the most potent natural phosphoantigen, (*E*)-4-hydroxy-3-methyl-but-2-enyl diphosphate (HMBPP) is produced by bacteria, but not humans (Morita et al., 2007). However, phosphoantigen-activated cells also can suppress viruses and malignancies (Gao et al., 2003; Wang et al., 2006).

Phosphoantigens such as HMBPP are detected by the Vγ9Vδ2 T cell receptor after binding to butyrophilin 3A1 (BTN3A1) (Harly et al., 2012; Wang et al., 2013) through major histocompatibility complex-independent mechanisms that are not yet completely clear. Both intracellular and extracellular binding of BTN3A1 to phosphoantigens have been recently reported (Sandstrom et al., 2014; Vavassori et al., 2013). Once activated, Vγ9Vδ2 T cells eliminate phosphoantigen-loaded target cells through killer cell lectin-like receptor subfamily K, member 1 receptor signaling and perforin release (Wrobel et al., 2007) and recruit other immune cells via chemokine production (Li et al., 2005, 2013). Therefore, development of compounds that can bind to BTN3A1 in cancer cells to promote their lysis by Vγ9Vδ2 T cells may be a promising anticancer strategy. However, questions remain about how to best target phosphoantigens to their cellular binding site.

Prodrug approaches increasingly are applied to compounds employed in antiviral and antitumor therapy (Hecker and Erion, 2008). The majority of prodrug applications of phosph(on)ates seek to facilitate passive diffusion through the cell membrane by masking negative charge until the compound is within the cell, eliminating the need for endocytic uptake. Because small, highly charged molecules can exhibit low membrane permeability (Kornberg et al., 1972), synthesis of protected compounds such as pivaloyloxymethyl (POM) derivatives (e.g., Adefovir dipivoxil) (Cundy, 1999; De Clercq, 2004; Marcellin et al., 2003) has been used to advance such molecules to clinical use. We hypothesized that an analogous strategy could be utilized to determine the role of cellular entry in phosphoantigen-induced T cell activation. Upon diffusion into the cell, the protecting groups from a phosphoantigen prodrug are thought to be released by cellular esterases, leaving an anionic phosphoantigen inside the cells. If intracellular/cytoplasmic binding to BTN3A1 is required for phosphoantigen activity, one might expect this strategy to increase potency relative to the free phosphoantigen anion, because the negatively charged phosphoantigen should not transverse the cell membrane as readily.

With this in mind, we developed a synthetic route to make POM-protected phosphoantigens and examined the activity of these compounds in Vγ9Vδ2 T cell activation. Here, we demonstrate that a POM-protected phosphoantigen is a highly potent Vγ9Vδ2 T cell stimulus, which effectively delivers the

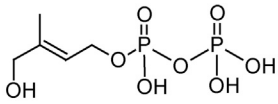

(*E*)-4-Hydroxy-3-methyl-but-2-enyl pyrophosphate, (HMBPP)

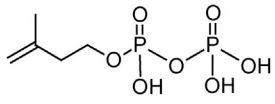

Isopentenyl diphosphate (IPP)

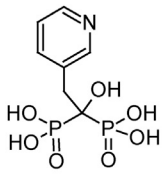

Risedronate

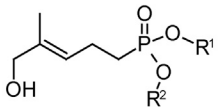

[(3*E*)-5-hydroxy-4-methylpent-3-en-1-yl]phosphonic acid, **1a**

Cmpd	-R^1	-R^2
1a	-H	-H
1b	-$H_2COC(O)C(CH_3)_3$	-$H_2COC(O)C(CH_3)_3$
1c	-$H_2COC(O)C(CH_3)_3$	-CH_3
1d	-CH_3	-CH_3

Figure 1. Chemical Structures of Phosphoantigens

Compounds evaluated in this study include the control phosphoantigens (HMBPP, IPP, and risedronate) and the phosphonate (**1a**), and its protected counterparts (**1b**, **1c**, and **1d**).

phosphoantigen to the intracellular binding site of BTN3A1. The compound, while nontoxic on its own, induces potent killing of malignant cells by Vγ9Vδ2 T cells, which could ultimately lead to a new class of cancer immunotherapy agents.

RESULTS

Synthesis of a Phosphoantigen and Its Pivaloyloxymethyl-Protected Prodrug

Vγ9Vδ2 T cells can be activated by direct phosphoantigens such as HMBPP, which can occur at low nanomolar concentrations, and indirect phosphoantigens such as the nitrogenous bisphosphonates, for which activation occurs at micromolar concentrations and is dependent upon their ability to increase the concentration of the direct phosphoantigen isopentenyl diphosphate (IPP) (Sicard et al., 2005) (Figure 1). However, diphosphates such as HMBPP have poor pharmacokinetic properties, most notably rapid clearance from the plasma due to phosphatase-mediated degradation and low membrane permeability due to the negative charges of the acidic oxygen atoms at physiological pH (Sicard et al., 2005). Therefore, we chose to generate a series of prodrug compounds based on the more stable phosphonate substructure (i.e., compound **1a**).

We have previously developed synthetic routes to make POM-protected bisphosphonates, which dramatically enhance cellular activity (Wiemer et al., 2008). To initiate the current synthetic pathway, we prepared the key phosphonate salt (compound **1a**) and the corresponding POM-modified compounds **1b** and **1c** (Figure 2). Phosphonate **1a** was chosen as our initial target because it has good chemical stability (decreasing the possibility of phosphatase metabolism) and is a modest phosphoantigen (Boëdec et al., 2008). However, to secure an efficient preparation of the parent structure as both the disodium salt **1a** and as the POM-protected compounds **1b** and **1c**, we developed the synthetic sequence shown in Figure 2. Thus after preparation of prenyl bromide **3** from alcohol **2**, this allylic halide was allowed to react with the anion of dimethyl methylphosphonate to afford the phosphonate **4**. Compound **4** was oxidized upon treatment with selenium dioxide, and then the *E* alcohol **1d** was isolated after treatment with $NaBH_4$ to reduce any aldehyde, using procedures we had applied earlier to preparation of geranyl (Kim et al., 2004) and then prenyl (Maalouf et al., 2007) derivatives. Hydrolysis of compound **1d** under standard conditions (McKenna et al., 1977) gave the expected sodium salt **1a** in good yield. Unfortunately, use of compound **1d** to prepare compound **1b** proved problematic. Because reaction at the hydroxyl group proved to be competitive, a slightly modified sequence was employed to reach compound **1b**. Phosphonate **4** first was converted to the bis-POM analog **6**. While some of the mono-POM mono-methyl ester **7** also was formed, this was not a significant complication because the two compounds were readily separable by column chromatography. Reaction of compound **6** with selenium dioxide gave the POM-protected target **1b** in modest yield. Compound **7** then was treated independently with selenium dioxide to obtain the closely related compound **1c**. Reduction with borohydride was avoided to minimize potential decomposition of the POM groups.

Pivaloyloxymethyl-Protected Phosphoantigens Potently Stimulate Human Peripheral Blood Vγ9Vδ2 T Cells

We evaluated compounds **1a** and **1b** for their ability to stimulate Vγ9Vδ2 T cell proliferation (Figure 3A). Peripheral blood mononuclear cells (PBMCs) derived from healthy donors were incubated with 1 μM of compound **1a** or **1b** for 3 days in the presence of interleukin 2 (IL-2). Cells were examined for the proportion of cluster of differentiation 3 (CD3)+ Vγ9Vδ2 T cells in live cultures 2 weeks post stimulation by flow cytometry. As expected, treatment with HMBPP (58.5% ± 1.8%) significantly expanded the population of Vγ9Vδ2 T cells as compared to cells treated with IL-2 alone (14.6% ± 3.7%). Compound **1a** was active at the reported concentrations (Table 1) (Boëdec et al., 2008). Interestingly, the POM prodrug (compound **1b**) was much more potent (57.7% ± 9.3%, at 1 μM) than compound **1a** and the activity approached the potency of HMBPP (Figure 3A). This is a key finding because it demonstrates a dramatic increase in activity through use of a phosphoantigen prodrug and supports an important role for intracellular delivery of phosphoantigens.

To examine further the activity of these compounds in stimulating human Vγ9Vδ2 T cells, compounds **1a** (unprotected), **1b** (two POM groups), **1c** (one POM group; one methyl group), and **1d** (two methyl groups) along with the known phosphoantigens HMBPP, IPP, and risedronate (Figure 3B and Figure S1 available online) were tested in a dose response manner. As expected, HMBPP potently expanded Vγ9Vδ2 T cells when stimulated for 3 days. At all of the tested concentrations (0.001–10 μM), HMBPP significantly increased Vγ9Vδ2 T cell population (Figure 3B), where HMBPP at 0.01 μM reached the peak of Vγ9Vδ2 T cell expansion to 63.3% ± 7.0%, which was more than a 4-fold increase compared to IL-2 alone treatment (14.6% ± 3.8%). The half maximal effective concentration (EC_{50}) of HMBPP in our hands was 0.00051 μM (Table 1).

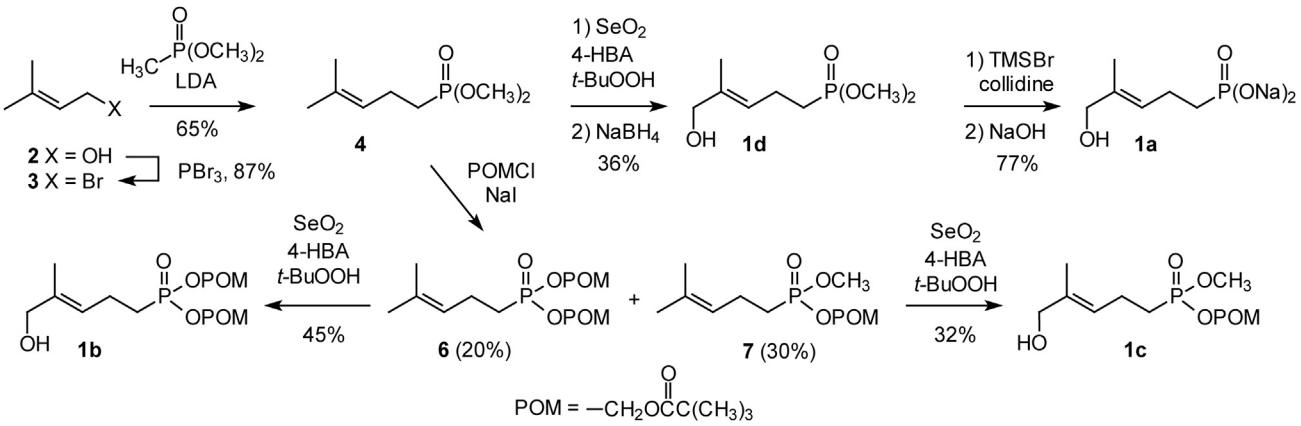

Figure 2. Synthesis of a Bis-Pivaloyloxymethyl Phosphoantigen Prodrug with Potent Expansion of Vγ9Vδ2 T Cells from Human Peripheral Blood

Synthetic pathways to compounds **1a**–**1d**.

Much higher levels of IPP are needed to trigger an IPP-specific Vγ9Vδ2 T cell response (Sireci et al., 2001). As expected, 1,000 μM IPP significantly expanded the Vγ9Vδ2 T cell population (Figure S2). The EC_{50} of IPP was 36 μM, approximately 70,000-fold less potent that HMBPP (Table 1). The nitrogen-containing bisphosphonate risedronate indirectly activates Vγ9Vδ2 T cell through inhibition of farnesyl diphosphate synthase and intracellular IPP accumulation (Thompson and Rogers, 2004). Consistently, risedronate increased the Vγ9Vδ2 T cell population in total PBMC cultures compared to treatment with IL-2 alone. Risedronate reached maximal stimulation at 10 μM (Figure S2). Risedronate at 1,000 μM, however, resulted in a significant reduction of the activity, most likely due to toxicity, similar to the effects observed with other nitrogen-containing bisphosphonates at concentrations above 100 μM (Miyagawa et al., 2001). To assess this toxicity, we measured cell viability at the day 14 time point and calculated half maximal inhibitory concentration (IC_{50}) values for each compound (Table 1). The selectivity indexes of HMBPP and risedronate were 980 and 38, respectively.

Consistent with a previous study (Boëdec et al., 2008), the sodium salt **1a** at 10 μM significantly increased the proportion of Vγ9Vδ2 T cells in the presence of IL-2, with an EC_{50} of 4 μM (Figure 3B; Table 1). Because dimethyl phosphonates are metabolically stable (Serafinowska et al., 1995), the dimethyl ester was predicted to be inactive and indeed compound **1d** did not show any stimulatory effect (Figure 3B; Table 1). Replacing one of the methyl groups with a labile POM group decreased the EC_{50} value to 0.5 μM (Table 1), and this compound (**1c)** at 1 μM was able to expand Vγ9Vδ2 T cell population to 51.1 ± 6.7% compared to 18.4 ± 5.4% from treatment with the dimethyl ester **1d** at 1 μM. Compound **1b,** which contains two POM groups, was much more potent than compounds **1a**, **1c,** and **1d**, providing an EC_{50} value of 0.0054 μM.Compound **1b** at 0.01 μM significantly expanded the Vγ9Vδ2 T cell population compared to IL-2 alone treatment and at 0.1 μM reached the peak of stimulation up to 62.9 ± 1.6% of Vγ9Vδ2 T cells in PBMC cultures, which was similar to the peak of Vγ9Vδ2 T cell expansion with 0.01 μM of the potent stimulator, HMBPP (63.3 ± 7.0%; EC_{50} = 0.00051 μM) (Figure 3B; Table 1). The EC_{50} of compound **1b** for T cell expansion was ~740x lower than that of compound **1a**, illustrating the vast improvement in efficacy seen by intracellular phosphoantigen delivery.

Pivaloyloxymethyl-Containing Compound 1b Is a Direct-Acting Phosphoantigen

Risedronate is known to stimulate Vγ9Vδ2 T cell proliferation by inhibition of farnesyl diphosphate (FPP) synthase in the mevalonate pathway, which results in accumulation of IPP. To determine whether the stimulatory effect of compound **1b** on Vγ9Vδ2 T cell proliferation could be caused by inhibition of FPP synthase and/or other enzymes of the mevalonate pathway, expansion of Vγ9Vδ2 T cells by risedronate and compound **1b** was compared in the presence or absence of lovastatin, which inhibits 3-hydroxy-3-methylglutaryl-coenzyme A reductase upstream of FPP synthase and prevents the synthesis of IPP. Treatment with 10 μM lovastatin alone did not alter the proliferation of Vγ9Vδ2 T cells. In the presence of 10 μM lovastatin, the stimulatory effect of risedronate at 10 μM on Vγ9Vδ2 T cell proliferation was significantly reduced from 48.9 ± 20.9% to 10.6 ± 4.0%. However, the stimulatory effect of compound **1b** on Vγ9Vδ2 T cell proliferation was not significantly affected in the presence of lovastatin (Figure 3C). The data demonstrate that prodrug **1b** does not achieve its stimulatory effect by altering the mevalonate pathway, but rather functions by releasing a direct phosphoantigen.

Only Compound 1b Significantly Induces Vγ9Vδ2 T Cell Proliferation after 2-hr Stimulation

Next, we assessed whether duration of the stimulation plays a role in the Vγ9Vδ2 T cell proliferation between different compounds. We hypothesized that enhanced uptake of compound **1b** would require a shorter stimulation time for maximal effects. Cells were treated with 0.1 μM HMBPP, 0.1 μM compound **1b**, 100 μM compound **1a**, or 100 μM risedronate for either 2 hr or the standard 3 days, followed by IL-2 supplementation every 3 days until day 14. Flow cytometry analysis showed that all compounds significantly expanded the Vγ9Vδ2 T cell population when the cells were stimulated for 3 days. In contrast, only

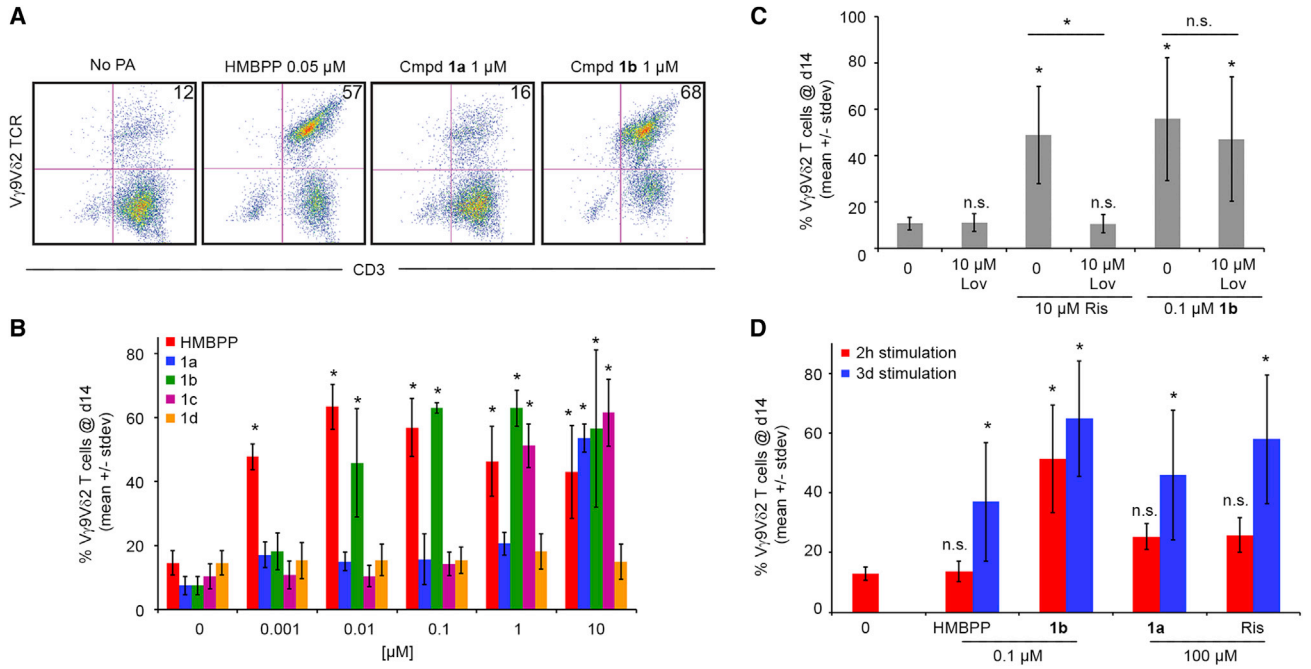

Figure 3. Bis-POM Prodrug 1b Functions as a Direct Phosphoantigen with Elevated Potency Relative to Free Acid 1a and HMBPP

(A) POM modification of a phosphoantigen increases cellular potency for activation of Vγ9Vδ2 T cells. Compounds **1a** and **1b** were used to stimulate proliferation for 3 days, and then removed. Cells were allowed to proliferate for 11 more days followed by staining for CD3 and the Vγ9Vδ2 TCR.

(B) Dose response curves for expansion of human peripheral blood Vγ9Vδ2 T cells by HMBPP and compounds **1a–1d** following a 3-day stimulation.

(C) Expansion of Vγ9Vδ2 T cells by compound **1b** is not blocked by cotreatment with lovastatin. Cells were stimulated as above with indicated concentrations of compound **1b** or risedronate in the presence or absence of 10 μM lovastatin.

(D) Cells were treated for either 2 hr or 3 days with HMBPP, risedronate, compound **1a,** or **1b** and expansion of Vγ9Vδ2 T cells was examined by flow cytometry. All data in (B)–(D) are represented as mean ± SD, n = 3, *p < 0.05 by ANOVA with Tukey's post-hoc analysis. See also Figure S1.

compound **1b** was able to significantly stimulate Vγ9Vδ2 T cell proliferation following a 2 hr-pulse treatment (Figure 3D). These observations indicate that compound **1b** is more effective in activating the Vγ9Vδ2 T cell population compared to all of the other compounds tested, including HMBPP.

The Butyrophilin 3A1 SPRY Associated Domain/sp1A/Ryanodine Receptor Domain, B30.2, Domain Directly Binds Phosphoantigens

It recently was reported that BTN3A1 is required for phosphoantigen detection by Vγ9Vδ2 T cells (Harly et al., 2012; Vavassori et al., 2013; Wang et al., 2013). However, the exact region of BTN3A1 where phosphoantigens bind is a matter of debate (Vavassori et al., 2013; Wang et al., 2013). Based on the 740x increase in activity of the bis-POM prodrug, we hypothesized that intracellular binding occurs, which is in contrast to the model of extracellular binding to the immunoglobulin-like V (IgV) (Vavassori et al., 2013). To determine whether the BTN3A1-antigen complex forms intracellularly or extracellularly, we expressed the recombinant extracellular IgV domain, the intracellular sp1A/ryanodine receptor domain/ SPRY associated domain (PRY/SPRY) (B30.2) domain, and the butyrophilin 3A1 full intracellular domain (BFI) and purified the soluble proteins. First, we verified the conformations of the constructs by nuclear magnetic resonance (NMR), and, according to the nicely dispersed ^{1}H-^{15}N-Heteronuclear Single Quantum Correlation (HSQC) spectra, all the recombinant proteins are well folded and remain in a monomeric state. Most of the amide resonance frequencies for PRY/SPRY domain overlapped with the peaks in the spectra for BFI (presented overlaid in Figure S4). This suggests the structure of PRY/SPRY domain in isolated form and in the context of the full-length protein remains the same and that the 68-residue membrane proximal region does not interact with the PRY/SPRY domain intramolecularly. We performed ITC to measure the interactions between these three BTN3A1 constructs and HMBPP (Figure 4A). While no binding was observed with the extracellular BTN3A1 IgV domain, both the intracellular PRY/SPRY (B30.2) domain and the BFI domain showed strong binding with dissociation constants (K_d) of 1.61 μM and 1.54 μM, respectively. The interaction of HMBPP with BTN3A1 was enthalpy-driven with an unfavorable entropy change. HMBPP binding to the full intracellular domain ($\Delta H = -51.9$ kJ/mol and $T\Delta S = -18.7$ kJ/mol) and the PRY/SPRY domain ($\Delta H = -49.4$ kJ/mol and $T\Delta S = -16.4$ kJ/mol) shares very similar enthalpy and entropy terms, which reveals the binding site on BTN3A1 for phosphoantigens is enclosed in the PRY/SPRY domain (Table S1). ^{1}H-^{15}N HSQC titrations of HMBPP agreed with the ITC results. While there were no chemical shift perturbations in the spectrum for the IgV domain upon HMBPP titration (Figure S5), the effects from HMBPP on the spectra of BFI and PRY/SPRY were very pronounced. HMBPP-concentration-dependent chemical shift perturbations were observed in the spectra for both BFI (Figure 5A)

Table 1. Activity of Compounds for Expansion of Vγ9Vδ2 T Cells from Human Peripheral Blood Mononuclear Cells and Inhibition of Cell Viability

Compound	EC_{50} (μM)	Fold difference from HMBPP	Fold difference from 1a[a]	IC_{50} (μM)	Selectivity index
HMBPP	0.00051	1.0	NA	0.50	980
IPP	36	71,000	NA	ND	ND
Risedronate	1.6	3,100	NA	61	38
1a	4.0	7,800	1	ND	ND
1b	0.0054	10	740	0.60	110
1c	0.50	980	8	8.6	17
1d	>10	>19,000	NA	ND	ND

NA, not applicable; ND, not determined.
[a]Compound **1a**

and the PRY/SPRY domain (Figure 5B) and reached saturation at an HMBPP:protein ratio of 3:1. Combining ITC and NMR data, we have demonstrated that HMBPP interacts with BTN3A1 at its intracellular domain at 1:1 ratio and is likely capable of inducing significant conformational rearrangements in the intracellular domain of BTN3A1.

To determine whether binding was specific to HMBPP or a general property of phosphoantigens, we also tested whether another potent phosphoantigen, (5-hydroxy-4-methylpent-3-enyl)-phosphonooxyphosphinic acid (C-HDMAPP) could bind to internal domain (Figure S2). C-HDMAPP is a phosphonate analog of HBMPP (Boëdec et al., 2008). Interestingly, C-HDMAPP exhibited similar energetics relative to HMBPP when binding to the PRY/SPRY domain (K_d = 1.95 μM, ΔH = −47.1 kJ/mol, TΔS = −14.5 kJ/mol). The data reveal that both HMBPP and C-HDMAPP bind with high affinity to the intracellular PRY/SPRY (B30.2) domain, but not the extracellular V domain. C-HDMAPP has a slightly weaker interaction, which is consistent with its activity in cellular assays (Boëdec et al., 2008). Therefore, we have demonstrated that two different phosphoantigens bind strongly to the intracellular domain of BTN3A1.

Because IPP also acts as a direct phosphoantigen in cellular assays, we tested its ability to interact with BTN3A1. However, we were unable to measure directly the binding of IPP to BTN3A1 by ITC. This is perhaps not surprising; given that the activity in cellular assays is approximately 71,000-fold less for IPP relative to HMBPP (Table 1), making the projected dissociation constant well outside of the detection limit of ITC. Therefore, we performed a competition ITC study to determine whether increasing concentrations of IPP would affect the binding of HMBPP to BTN3A1 (Figure S4). IPP dose-dependently decreased the favorable enthalpy of HMBPP binding from a ΔH of −51.9 kJ/mol to −47.7 kJ/mol and −38.7 kJ/mol at IPP:BTN3A1 ratios of 10:1 and 100:1, respectively (Table S1). IPP also dose-dependently made more favorable the TΔS term of HMBPP binding, changing it from −18.7 kJ/mol to −12.7 kJ/mol and −6.78 kJ/mol at IPP:BTN3A1 ratios of 10:1 and 100:1 respectively. Taken together, the data show that IPP binds to BTN3A1 with a much weaker affinity compared to HMBPP and that both compounds compete for the same binding site within the PRY/SPRY domain.

Because compound **1b** is expected to undergo metabolic cleavage, resulting in accumulation of compound **1a**, we examined the binding affinity between compound **1a** and the BTN3A1 PRY/SPRY domain. Like IPP, the binding affinity of **1a** was undetectable in ITC when using compound **1a** as the sole ligand, as we had purposely chosen a weak phosphoantigen for the prodrug studies. However, as expected, compound **1a** had a markedly stronger effect on the HMBPP binding to the PRY/SPRY domain relative to IPP (Figure 4B). Like IPP, compound **1a** dose-dependently decreased the favorable enthalpy of HMBPP binding to BTN3A1. These effects also were measured at **1a**:BTN3A1 ratios of 0:1(ΔH of −51.9 kJ/mol), 10:1 (−49.1 kJ/mol), and 100:1 (−28.5 kJ/mol). Compound **1a** also dose-dependently made more favorable the TΔS term of HMBPP binding at IPP:BTN3A1 ratios of 10:1 (−16.2 kJ/mol) and 100:1 (+5.19 kJ/mol). These data fit well with the cellular data in that **1a** is a more potent phosphoantigen relative to IPP and would be expected to have a stronger effect. Perhaps surprisingly, the entropy term became positive at the highest concentration of **1a**. This finding demonstrates that the prenyl alcohol and/or the olefin position play a more important role in the phosphoantigen-BTN3A1 interaction as compared to the distal phosphate group. Thus, according to ITC data, compound **1a** may induce conformational changes in the intracellular domain of BTN3A1 similar to the ones induced by the stronger interaction with HMBPP and absent in the interface with IPP.

To confirm that IPP and compound **1a** do have direct interactions with the intracellular domain of BTN3A1, ^{1}H-^{15}N HSQC titrations of IPP and compound **1a** into BFI were performed at ligand:protein molar ratios of 0:1, 10:1, and 100:1. Both IPP (Figure S6A) and compound **1a** (Figure S6B) showed concentration-dependent perturbations in the spectra. These two sets of titration data demonstrate that both IPP and compound **1a** bind to BFI at a similar binding site with only a limited number of distinct differences in amide chemical shift perturbations between the two. In addition, the spectrum of compound **1a**, but not IPP, shows several chemical shift perturbations identical to the ones observed in the titration of HMBPP (marked by arrows on Figure S6C). Thus our NMR and ITC results are mutually consistent and suggest that binding sites for IPP and compound **1a** on the PRY/SPRY domain are quite similar, although each compound is also involved in unique interactions with BTN3A1.

Prodrug 1b Stimulates Lysis of Daudi Lymphoma Cells by Vγ9Vδ2 T Cells

To examine if compound **1b** can induce T cell killing of malignant cells, we examined the extent of Vγ9Vδ2 T cell lysis of Daudi lymphoma cells. Daudi cells were labeled with a fluorescent cell membrane dye and mixed with purified Vγ9Vδ2 T cells at a ratio of 5 to 1. Following coculture in the presence or absence of 0.1 μM test compounds, cells were stained with fluorescein isothiocyanate (FITC)-Annexin V antibody and the cell profiles examined by flow cytometry. The Vγ9Vδ2 T cells in combination with compound **1b** resulted in a significant increase in Annexin V positive Daudi cells in comparison to no phosphoantigen treatment (Figure 6A). Of the test compounds, only HMBPP and compound **1b** resulted in significant increase in Annexin V positive Daudi cells (Figure 6B), with compound **1b** promoting greater T cell cytotoxic activity than HMBPP. In the absence of

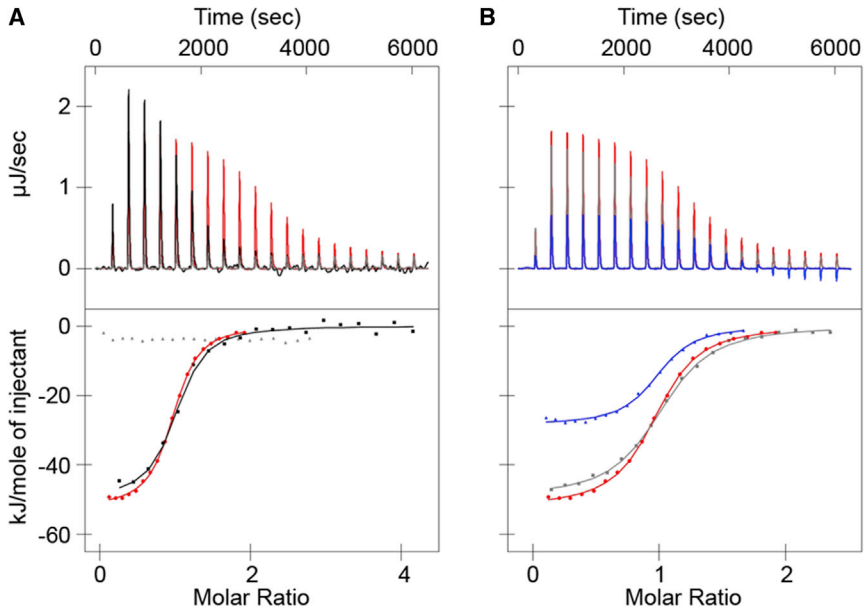

Figure 4. Binding of HMBPP and Compound 1a to the Intracellular Domain of BTN3A1

(A) Isothermal titration calorimetry plots for the interaction of HMBPP with the extracellular IgV domain (gray line/dots), the full intracellular domain (BFI) (black line/dots), or the isolated PRY/SPRY (B30.2) domain (red line/dots).

(B) Isothermal titration calorimetry plots for the interaction of the full intracellular domain (BFI) of BTN3A1 with HMBPP in the absence of compound **1a** (red line/dots), or the presence of 10x compound **1a** (gray line/dots), or 100x compound **1a** (blue line/dots).

See also Figures S2 and S3 and Table S1.

T cells, no effect on the viability of Daudi cells was observed when the cells were treated with high concentrations of either compound **1a** or **1b** (Figure 6C) for up to 72 hr at 10 μM. In contrast, cell viability was significantly reduced when treated with vorinostat.

DISCUSSION

In this study we have described the synthesis and evaluation of a phosphoantigen prodrug. Surprisingly, this compound exhibits a large increase in potency relative to the free phosphoantigen and displays similar, if not greater, potency relative to HMBPP. Additionally, our analysis of the newly synthesized POM-modified prodrug highlights several important conclusions (Figure 6D) about the mechanisms that underlie phosphoantigen presentation: (1) phosphoantigen charge serves as a barrier to both cellular entry and exit, (2) phosphoantigens bind to the intracellular, and not extracellular, domain of BTN3A1, and (3) effective delivery of phosphoantigens to the cytoplasm of malignant cells induces their lysis by Vγ9Vδ2 T cells.

At the start of our studies, the molecular target of phosphoantigens was not known, so we had deliberately chosen to combine a moderate strength phosphoantigen with a well characterized prodrug to ensure that we could measure any potency increases generated by the prodrug strategy. To that end, it was quite surprising to see that compound **1b** rivals the potency of HMBPP, the most potent known phosphoantigen. Additionally, relative to the free phosphonic acid **1a**, the pivaloyloxymethyl prodrug **1b** is approximately 750 times more potent for expansion of Vγ9Vδ2 T cells from peripheral blood following a three day stimulation (Table 1). The increased activity is even more prevalent in assays using shorter incubation times (Figure 3D), such as the two hour PBMC stimulation or the four hour Daudi lysis assay (Figure 6B). In both of these assays, strong activity was seen with 0.1 μM of compound **1b**, while the activity of the free phosphonic acid **1a** at this concentration was not measureable. These results demonstrate that phosphoantigen neutralization dramatically decreases the time necessary for loading phosphoantigen presenting cells and suggest that charged phosphoantigens enter cells primarily by active uptake rather than passive diffusion. There is clearly an opportunity for further increases in potency, which could be generated either though utilizing stronger phosphoantigens as templates or through utilizing different prodrug motifs.

During the course of these studies, two groups reported binding of phosphoantigens to BTN3A1 via conflicting mechanisms (Sandstrom et al., 2014; Vavassori et al., 2013). Initially, De Libero and colleagues (Vavassori et al., 2013) demonstrated extracellular binding, whereas a recent paper by Adams (Sandstrom et al., 2014) clearly showed intracellular binding. Our studies are in strong agreement with those from the Adams Laboratory. In addition to the calorimetry assay, we also see strong interactions as assessed by NMR spectroscopy. Our results also demonstrate the relative contribution of the prenyl alcohol group and/or olefin position is more important than the second phosphate group, because binding of HMBPP to BTN3A1 is more strongly affected by **1a** than IPP. Additionally, we have compared the effects of different antigen binding on the full intracellular domain and the PRY/SPRY domain by NMR. Our results indicate that although the binding site for phosphoantigens is localized in PRY/SPRY domain, the 68-residue membrane proximal region, preceding PRY/SPRY, also undergoes major structural rearrangement upon binding (Figure 5C). In the future, it will be interesting to determine the molecular details and the role of the lipid bilayer in this process. While we are still in process of resonance assignments, which can be time consuming for a protein of this size, our data are consistent with the recently published crystal structure of the PRY/SPRY domain in complex with HMBPP (Sandstrom et al., 2014). Our findings clearly promote a model in which intracellular binding of phosphoantigens to BTN3A1 induces a conformational change, which either propagates across the membrane to the extracellular region or promotes an interaction with another intracellular protein, thus allowing new transmembrane complex formation necessary for recognition by the Vγ9Vδ2 T cell receptor.

Phosphoantigen prodrugs such as these may ultimately become clinically useful. Currently, there has been only one

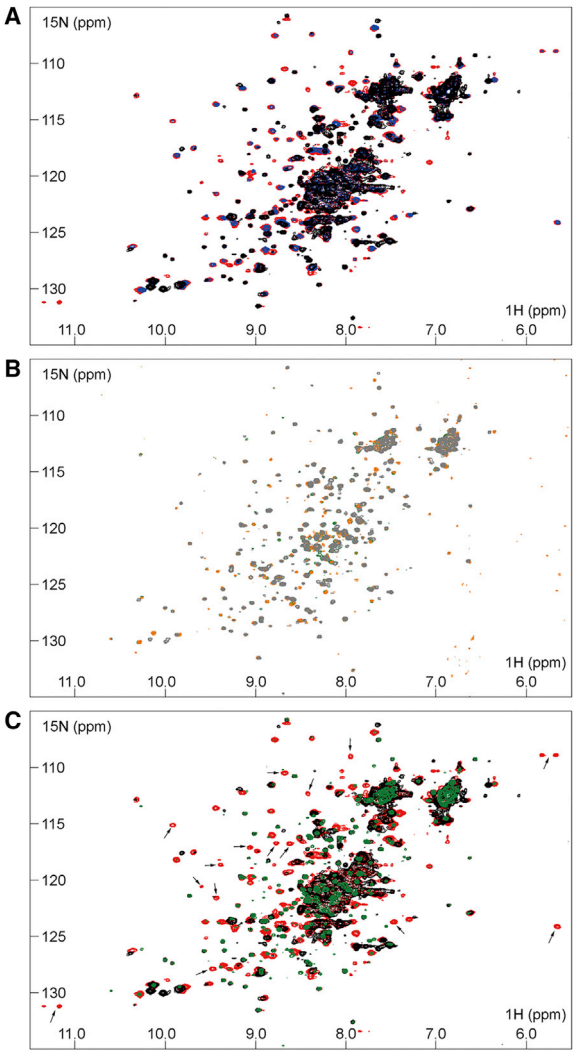

Figure 5. ^{1}H-^{15}N HSQC Titration of HMBPP into the Full-Length Intracellular Domain and the PRY/SPRY Domain of BTN3A1

Compared to the PRY/SPRY domain, the full-length intracellular domain of BTN3A1 (BFI) includes an additional membrane-proximal region of 68 residues at the N terminus, which is demonstrated to be involved in the interaction with HMBPP and to undergo significant structural changes upon binding.

(A) Chemical shift perturbations for the interaction of HMBPP and BFI at ratios of 0:1 (black), 1:1 (blue), and 3:1 (red).

(B) Chemical shift perturbations for the interaction of HMBPP and the PRY/SPRY domain at ratios of 0:1 (gray), 1:1 (orange), and 3:1 (green).

(C) Evidence for the involvement of the 68-residues membrane-proximal region in interaction with HMBPP: HSQC spectra of the free BFI (black), BFI + HMBPP at 1:3 ratio (red), and PRY/SPRY + HMBPP at 1:3 ratio (green). Peaks that belong to the 68-residue membrane-proximal region are absent in the spectrum of PRY/SPRY domain. Arrows indicate the peaks corresponding to the amides from this region that have showed remarkable shifts upon binding to HMBPP, thus suggesting significant structural rearrangements.

See also Figures S4–S6.

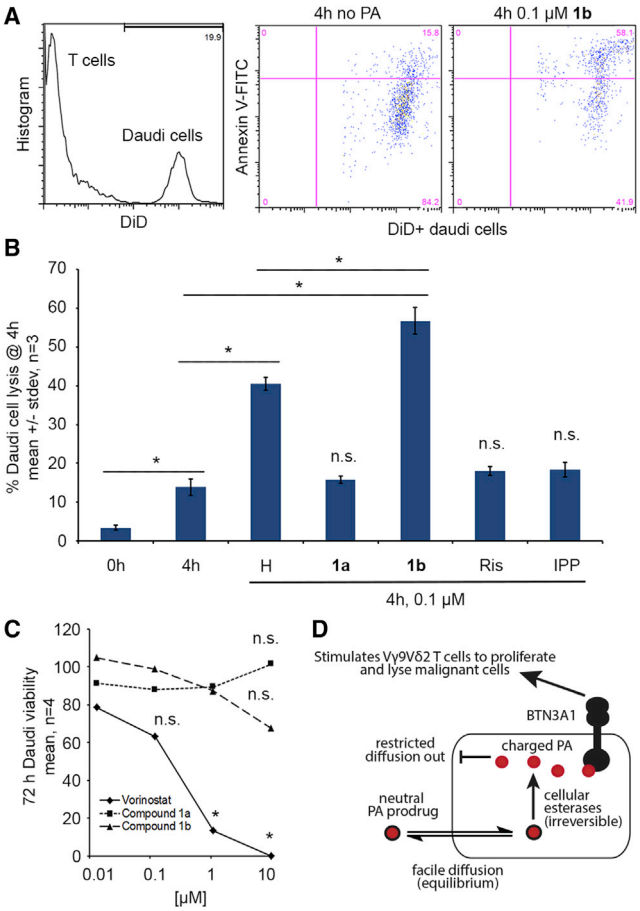

Figure 6. Bis-POM Prodrug 1b Promotes Lysis of Daudi Lymphoma Cells by Vγ9Vδ2 T Cells

(A) DiD labeled Daudi cells were cocultured for 4 hr in the presence of Vγ9Vδ2 T cells at a 1:5 ratio and assessed by annexin V-FITC staining. Treatment with compound **1b** increases the number of annexin V positive Daudi cells.

(B) The mixture was incubated with various test compounds at 0.1 μM. Data are represented as mean ± SD, n = 3, *p < 0.05 by ANOVA with Tukey's post-hoc analysis.

(C) 72 hr viability of Daudi cells incubated with compounds **1a** and **1b** relative to vorinostat as a positive control. The mean of four replicates is presented, *p < 0.05 by ANOVA with Tukey's post-hoc analysis.

(D) A proposed prodrug model illustrates pathways for POM-modified compound internalized and presented by antigen presenting cells. Charged molecules such as phosph(on)ates have restricted membrane diffusion. By neutralizing charge with a cell cleavable protecting group, one can encourage diffusion into cells, and upon intracellular release ion trapping results in elevated intracellular levels.

direct phosphoantigen that has been tested in human clinical trials, 4-bromo-3-hydroxy-3-methylbutyl diphosphate (BrHPP) (Fournié et al., 2013). In these trials, the initial stimulation led to an expansion of the Vγ9Vδ2 population, but this required large intravenous doses and was limited in subsequent cycles of therapy. This dosing regimen was likely a consequence of limited plasma stability of BrHPP (a diphosphate), because studies in primates demonstrated rapid degradation in the plasma (Sicard et al., 2005). Our results clearly show a time dependency to the uptake of phosphoantigens by peripheral blood cells, with no activation seen with HMBPP treatment of two hours (Figure 3D). This explains the fact that a very high concentration of BrHPP was needed to see any activation of Vγ9Vδ2 T cells in these patients. We have shown that the phosphoantigen prodrug **1b** requires a much shorter incubation time. Therefore, this or other

similar neutral compounds may be able to achieve Vγ9Vδ2 T cell activation in human blood with significantly lower doses relative to BrHPP.

Alternatively, others have used bisphosphonate drugs as phosphoantigens in clinical trials (Van Beek et al., 2002); however, these compounds also have severely restricted pharmacokinetics (e.g., rapid bone sequestration), low therapeutic indexes, and the potential for side effects such as osteonecrosis. Our data (Table 1) clearly show the advantage of using direct phosphoantigens over an indirect phosphoantigen, as HMBPP has a selectivity index that is 25 times greater than risedronate. It is not clear whether other nitrogenous bisphosphonates, such as zoledronate, have similarly narrow selectivity indexes. However, we presume this to be the case as both the stimulation and the cytotoxicity result from cellular inhibition of FPP synthase, and at least one other group, has reported that shorter durations of stimulation with zoledronate reduces its cytotoxic effects (Nussbaumer et al., 2013). Compound **1b** also has an improved selectivity index relative to risedronate, and again we believe it to be possible to make further gains in this area through compound optimization.

Finally, it is important to note the functional consequences of the phosphoantigen prodrug in the inducible lysis of cancer cells (Figure 6). Compound **1b** causes no discernable growth inhibition of Daudi cells at concentrations up to 10 μM and treatment times up to 72 hr. However, when combined with Vγ9Vδ2 T cells, compound **1b** can induce the lysis of Daudi cells at 0.1 μM in only four hours. Therefore, we believe that compounds such as **1b**, if effectively delivered to malignant cells, have the potential for strong chemically induced cancer immunotherapy through recruiting a targeted Vγ9Vδ2 T cell response.

In conclusion, these findings reveal several key mechanisms of antigen recognition in the immune system and point to new possibilities for development of clinical agents through understanding phosphoantigen structure activity relationships at the molecular and cellular levels.

SIGNIFICANCE

We have described a phosphoantigen prodrug that functions with exquisite potency. The prodrug defines key roles of phosphoantigen charge, binding, and delivery. This strategy has potential to impact clinical use of phosphoantigens, which have been limited by poor pharmacokinetics, for treatment or prevention of cancer and infectious disease.

EXPERIMENTAL PROCEDURES

Chemical Synthesis

Compound 4

To a stirred solution of *n*-BuLi (2.4 M in hexanes, 14.6 ml, 35.0 mmol) in tetrahydrofuran at −78°C was added *N,N*-diisopropyl amine (4.82 ml, 34.4 mmol). The resulting solution was allowed to stir for 10 min and dimethyl methylphosphonate (3.7 ml, 34.1 mmol) was added slowly via syringe. Once addition was complete, the mixture was allowed to stir for 15 min during which time a white precipitate formed. Prenyl bromide **3** (5.17 g, 34.7 mmol) was added slowly via syringe, and after addition was complete the solution was allowed to stir for an additional 30 min at –78°C, allowed to warm to room temperature unassisted, and stirred overnight. A saturated aqueous solution of NH_4Cl was added, the solution was extracted with Et_2O, and the combined extracts were dried (Na_2SO_4) and concentrated in vacuo. Final purification was achieved using flash column chromatography (3% MeOH in Et_2O) to afford the target compound in 65% yield (4.31 g) as a clear oil: ^{1}H NMR δ 5.07–5.00 (m, 1H), 3.67 (d, J_{HP} = 11.1 Hz, 6H), 2.26–2.14 (m, 2H), 1.75–1.63 (m, 2H), 1.62 (s, 3H), 1.55 (s, 3H); ^{13}C NMR δ 132.9, 123.1 (d, J_{CP} = 16.7 Hz), 52.2 (2C), 25.7, 25.0 (d, J_{CP} = 137.9 Hz), 21.1 (d, J_{CP} = 4.8 Hz), 17.7; ^{31}P NMR δ 34.2; high resolution mass spectrometry (HRMS) (time-of-flight [TOF] MS electron impact [EI]) *m/z* calculated for $C_8H_{18}O_3P$ $(M+H)^+$ 193.0994, found 193.0973.

Compound 1d

To a vigorously stirred solution of compound **4** (2.03 g, 10.6 mmol) in CH_2Cl_2 at room temperature were added SeO_2 (0.602 g, 5.4 mmol), 4-hydroxy benzoic acid (0.150 g, 1.1 mmol), and *t*-BuOOH (70% in H_2O, 5.48 ml, 42.6 mmol). The solution was allowed to stir for 19 hr and a saturated aqueous solution of $NaHCO_3$ was added. The solution was extracted (CH_2Cl_2), and the combined extracts were dried ($MgSO_4$) and concentrated in vacuo. The crude material was dissolved in MeOH with stirring, cooled to 0°C in an ice bath, and $NaBH_4$ (0.820 g, 21.6 mmol) was added in several aliquots. The solution was allowed to stir for 2.5 hr, saturated aqueous NH_4Cl was added, the solution was extracted (Et_2O), and the combined extracts were dried ($MgSO_4$) and concentrated in vacuo. Final purification by flash column chromatography (6%–10% MeOH in Et_2O) afforded the target compound in 36% yield (0.781 g) as a clear oil: ^{1}H NMR δ 5.37–5.31 (m, 1H), 3.89 (s, 2H), 3.66 (d, J_{HP} = 11.7 Hz, 6H), 2.32–2.19 (m, 2H), 1.79–1.68 (m, 2H), 1.58 (s, 3H); ^{13}C NMR δ 136.3, 122.8 (d, J_{CP} = 15.7 Hz), 67.5, 52.1 (d, J_{CP} = 6.9 Hz, 2C), 24.3 (d, J_{CP} = 138.6 Hz), 20.2 (d, J_{CP} = 4.6 Hz), 13.3; ^{31}P NMR δ 34.3; HRMS (TOF MS EI) *m/z* calculated for $C_8H_{17}O_4PNa$ $(M+Na)^+$ 231.0762, found 231.0745.

Compound 1a

Compound **1d** (0.166 g, 0.80 mmol) was dissolved in CH_2Cl_2, and the mixture was cooled to 0°C in an ice bath. Collidine (0.425 ml, 3.2 mmol) and bromotrimethylsilane (0.419 ml, 3.2 mmol) were added via syringe, and the reaction was allowed to stir overnight. After the volatiles were removed, toluene was added and removed in vacuo, and this cycle was repeated three times providing a white solid. The solid was dissolved in an aqueous NaOH (1.49 M, 2.15 ml, 3.2 mmol), and the reaction mixture was stirred overnight. The mixture was poured into an equal volume of acetone and cooled at 7°C for a period of 24 hr to facilitate precipitation. Acetone and H_2O were removed in vacuo, the resulting solid was washed with acetone, dissolved in H_2O, and washed with diethyl ether. The aqueous phase was decolorized using activated charcoal and concentrated in vacuo to provide the target salt in 77% yield (137 mg): ^{1}H NMR δ 5.52–5.45 (m, 1H), 3.94 (broad singlet [br s], 2H), 2.23–2.11 (m, 2H), 1.64 (br s, 3H), 1.45–1.33 (m, 2H); ^{13}C NMR δ 134.0, 128.6 (d, J_{CP} = 17.3 Hz), 67.9, 29.5 (d, J_{CP} = 126.9 Hz), 22.92, 13.5; ^{31}P NMR δ 22.3; HRMS (TOF MS EI) *m/z* calculated for $C_6H_{12}O_4P$ $(M-H)^-$ 179.0473, found 179.0460.

Compounds 6 and 7

Phosphonate **4** (0.967 g, 5.0 mmol), sodium iodide (1.56 g, 10.4 mmol), and pivaloyloxymethyl chloride (2.3 ml, 15.9 mmol) were added to acetonitrile under an atmosphere of argon. The mixture was heated and held at reflux with vigorous stirring overnight. Water and diethyl ether were added, and the phases were separated. The aqueous phase was extracted with diethyl ether, and the combined organic extracts were dried (Na_2SO_4) and concentrated in vacuo. Final purification by flash column chromatography (30% Et_2O in hexanes to 50% Et_2O in hexanes) gave the target compound in 20% yield (391 mg) as a clear oil: ^{1}H NMR δ 5.60 (d, J_{HP} = 13.2 Hz, 4H), 5.04–4.97 (m, 1H), 2.26–2.14 (m, 2H), 1.84–1.71 (m, 2H), 1.61 (s, 3H), 1.53 (s, 3H), 1.16 (s, 18H); ^{13}C NMR δ 176.6 (2C), 133.0, 122.2 (d, J_{CP} = 17.9 Hz), 81.1 (d, J_{CP} = 6.5 Hz, 2C), 38.6 (2C), 26.6 (d, J_{CP} = 136.8 Hz), 26.7 (6C), 25.4, 20.5 (d, J_{CP} = 4.6 Hz), 17.5; ^{31}P NMR δ 32.7; HRMS (TOF MS EI) *m/z* calculated for $C_{18}H_{33}O_7PNa$ $(M+Na)^+$ 415.1862, found 415.1868.

Compound **6** was accompanied by compound **7** and isolated in 30% yield (0.46 g) as a clear oil: ^{1}H NMR (300 MHz, $CDCl_3$) δ 5.67 (d, J_{HP} = 13.4 Hz, 2H), 5.14–5.05 (m, 1H), 3.75 (d, J_{HP} = 11.1 Hz, 3H), 2.36–2.20 (m, 2H), 1.91–1.74 (m, 2H), 1.68 (s, 3H), 1.62 (s, 3H), 1.24 (s, 9H); ^{13}C NMR (75 MHz, $CDCl_3$) δ 176.6 (s), 134.7 (d, J_{CP} = 1.8 Hz), 122.4 (d, J_{CP} = 17.4 Hz), 81.4 (d, J_{CP} = 5.9 Hz), 51.5 (d, J_{CP} = 7.0 Hz), 38.4 (s), 26.6 (s, 3C), 25.3 (s), 25.0 (d, J_{CP} = 35.1 Hz), 20.2 (d, J_{CP} = 4.8 Hz), 17.3 (s); ^{31}P NMR (121 MHz, $CDCl_3$) 33.7; HRMS (ESI^+) *m/z* calculated for $C_{13}H_{25}O_5PNa$ $(M+Na)^+$ 315.1337, found: 315.1337.

Compound 1b

Compound **6** (0.361 g, 0.92 mmol) was dissolved in CH_2Cl_2 followed by addition of SeO_2 (0.05 g, 0.45 mmol), *t*-BuOOH (70% aqueous, 0.47 ml, 3.65 mmol), and 4-hydroxybenzoic acid (0.013 g, 0.094 mmol). The mixture was stirred vigorously overnight and then an aqueous solution of saturated $NaHCO_3$ was added. The mixture was extracted with CH_2Cl_2, the combined organic extracts were dried (Na_2SO_4), and concentrated in vacuo. Final purification by flash column chromatography (10% hexanes in Et_2O) afforded the target product in 45% yield (168 mg) as a clear oil: ^{1}H NMR δ 5.60 (d, J_{HP} = 12.9 Hz, 4H), 5.34–5.28 (m, 1H), 3.91 (br s, 2H), 2.34–2.19 (m, 2H), 1.89–1.77 (m, 2H), 1.58 (s, 3H), 1.17 (s, 18H); ^{13}C NMR δ 176.9 (2C), 136.6, 122.7 (d, J_{CP} = 15.7 Hz), 81.2 (d, J_{CP} = 6.2 Hz, 2C), 67.9, 38.6 (2C), 26.4 (d, J_{CP} = 138.2 Hz), 26.7 (6C), 20.2 (d, J_{CP} = 5.2 Hz), 13.5; ^{31}P NMR 32.6; HRMS (TOF MS EI) *m/z* calculated for $C_{18}H_{34}O_8P$ $(M+H)^+$ 409.1992, found 409.1995.

Compound 1c

Compound **7** (0.45 g, 1.54 mmol), SeO_2 (0.09 g, 0.77 mmol), 4-hydroxybenzonic acid (0.02 g, 0.15 mmol), and *t*-BuOOH (0.79 ml, 6.15 mmol) were dissolved in dichloromethane (10 ml), and the reaction was allowed to stir overnight. The solution was quenched by addition of water and extracted with diethyl ether. The organic portions were combined and washed with brine and aqueous sodium thiosulfate, the solution was dried ($MgSO_4$), filtered, and concentrated in vacuo. The residue was purified via flash chromatography (ether), and the desired product **1c** was isolated as a yellow oil in 32% yield (0.15 g, 43% based on recovered starting material): ^{1}H NMR (300 MHz, $CDCl_3$) 5.71–5.61 (m, 2H), 5.44–5.34 (m, 1H), 3.98 (s, 2H), 3.75 (d, J_{HP} = 11.3 Hz, 3H), 2.85 (br s, 1H), 2.38–2.28 (m, 2H), 1.92–1.81 (m, 2H), 1.66 (s, 3H), 1.24 (s, 9H); ^{13}C NMR (75 MHz, $CDCl_3$) δ 177.0 (s), 136.4 (d, J_{CP} = 1.4 Hz), 122.9 (d, J_{CP} = 16.2 Hz), 81.5 (d, J_{CP} = 6.3 Hz), 67.8 (s), 51.8 (d, J_{CP} = 7.2 Hz), 38.6, 26.8 (s, 3C), 26.6 (d, J_{CP} = 20.3 Hz), 20.3 (d, J_{CP} = 4.8 Hz), 13.5 (s); ^{31}P NMR (121 MHz, $CDCl_3$) 33.5; HRMS (ESI^+) *m/z* calculated for $C_{13}H_{25}O_6PNa$ $(M+Na)^+$ 331.1286, found: 331.1291.

Vγ9Vδ2 T Cell Isolation and Culture

Human peripheral blood mononuclear cell (PMBCs) were isolated from blood from Research Blood Components using density centrifugation. Cells were frozen in freezing media (10% DMSO, 90% fetal bovine serum [FBS]) in liquid nitrogen until needed. $2-4 \times 10^6$ cells were resuspended in fresh T cell media (RPMI-1640, 10% heat-inactivated FBS, 1x 4-(2-hydroxyethyl)-1-piperazineethanesulfonic acid, pyruvate, nonessential amino acids, β-mercaptoethanol [BME]) and added to 6-well plates. Cells were stimulated for 3 days unless stated otherwise. Cells were cultured for another 11 days after compound removal. Human IL-2 (5 ng/ml) was supplemented every 3 days. All experiments were performed at least three times independently using at least two different blood donors.

Flow Cytometry

Cells were washed and suspended in 100 μl of fluorescence-activated cell sorting buffer (2% BSA in PBS). Total gamma delta T cell receptor (TCR) was labeled using either FITC-anti-human Pan gamma delta TCR antibody or anti-human Pan gamma delta TCR antibody followed by peridinin chlorophyll-eFluor 710-anti-mouse immunoglobulin G1. Cells were costained with PE-conjugated anti-human CD3. Each step was done at 4 degrees for 30 min, washed twice, and then fixed in 3% paraformaldehyde before flow analysis. Data were analyzed using FlowJo.

Cloning and Purification of Butyrophilin 3A1 Constructs

BTN3A1 constructs were purified based on the method that De Libero and colleagues (Vavassori et al., 2013) with some modifications (see Supplemental Experimental Procedures).

Isothermal Titration Calorimetry

Calorimetric measurements of BTN3A1 domains were performed on a low volume Nano ITC. All experiments were carried out in a buffer of 50 mM Tris, pH 7.5, 100 mM NaCl, 5 mM BME at 25°C with a stirring speed of 200 rpm to minimize the precipitation. Each titration consisted of twenty 2.5 μl injections with 300 s time intervals. The concentrations of protein samples were determined by UV, and the compounds were prepared in the same buffer from the dilution of 10 mM or 100 mM stock. The protein concentration ranged from 30 μM to 60 μM. The concentration of protein was examined after each ITC experiment and a good solubility (>85%) was shown. Data analysis was done in NanoAnalyze Software suite using an "independent" model. In all cases, a stoichiometry of 1 ± 0.1 was revealed.

Nuclear Magnetic Resonance Spectroscopy

^{15}N-labeled recombinant proteins were overexpressed in M9 medium supplemented with $^{15}NH_4Cl$ as the sole nitrogen source and purified as above. NMR samples of 100–200 μM were prepared in a buffer of 50 mM Tris, pH 7.5, 100 mM NaCl, 5 mM BME, 7% D_2O, 1 mM 4,4-dimethyl-4-silapentane-1-sulfonic acid as the internal standard. ^{1}H-^{15}N HSQC titration experiments were performed on Varian Inova 600 MHz spectrometer equipped with inverse-triple resonance cryoprobe at 25°C. All spectra were processed with NMRPipe (Delaglio et al., 1995) and analyzed in CcpNmr Analysis (Vranken et al., 2005) software suite.

Daudi Killing Assay

The Daudi killing assay was performed based on (Gomes et al., 2010) with slight modification. Vγ9Vδ2 T cells were expanded from PMBCs by stimulation with 0.01 μM HMBPP for 3 days and expansion for 8−11 additional days as above. At that time, Vγ9Vδ2 T cells were purified by negative selection using a kit. Resulting populations were typically 98%−99% Vγ9Vδ2 T cells as assessed by flow cytometry. Daudi cells were stained with DiD (2 min in 4 μM DiD in BSA/PBS), quenched by addition of an equal volume of FBS, and washed twice in T cell media. Daudi cells (6×10^3) were mixed with 3×10^4 T cells and test compounds to a final volume of 100 μl. Mixtures were incubated for 4 hr at 37 degrees then placed on ice for 5 min. Annexin V FITC (3 μl) was added for 15 min on ice, then cells were diluted by addition of 200 μl binding buffer (Becton Dickinson) and immediately analyzed by flow cytometry.

Proliferation Assay

Daudi proliferation was performed as described with the following parameters (Wiemer et al., 2013). Cells/well (10,000) were added to 96-well plates in 100 μl in the presence of test compounds. Cells were allowed to proliferate for 72 hr. During the last 2 hr, cells were labeled with 5 μl of CellQuantiBlue reagent and were scanned with a Victor plate reader.

Statistical Analysis

One-way ANOVA was used to calculate significance. Comparisons were done relative to the control or between pairs of conditions. Columns in bar graphs represent the mean ± SD. An α level of 0.05 was used.

SUPPLEMENTAL INFORMATION

Supplemental Information includes Supplemental Experimental Procedures, six figures, and one table and can be found with article online at http://dx.doi.org/10.1016/j.chembiol.2014.06.006.

AUTHOR CONTRIBUTIONS

C-H.C.H. and A.J.W. performed molecular biology and cell-based experiments. R.J.B. and R.R.S. performed the chemical synthesis under supervision of D.F.W. Protein purification, ITC, and HSQC NMR were performed by X.L. under supervision of O.V. Cell viability experiments were performed by J.L. The manuscript was written by C-H.C.H. and A.J.W. with the support of X.L, O.V., and D.F.W.

ACKNOWLEDGMENTS

Financial support from the University of Connecticut Department of Pharmaceutical Sciences (A.J.W.) and from the Roy J. Carver Charitable Trust as a Research Program of Excellence (D.F.W.) is gratefully acknowledged. A.J.W. and D.F.W. are cofounders of Terpenoid Therapeutics, and D.F.W. is on its Board. The current work did not involve the company.

Received: April 24, 2014
Revised: June 12, 2014
Accepted: June 18, 2014
Published: July 24, 2014

REFERENCES

Boëdec, A., Sicard, H., Dessolin, J., Herbette, G., Ingoure, S., Raymond, C., Belmant, C., and Kraus, J.L. (2008). Synthesis and biological activity of phosphonate analogues and geometric isomers of the highly potent phosphoantigen (E)-1-hydroxy-2-methylbut-2-enyl 4-diphosphate. J. Med. Chem. *51*, 1747–1754.

Bonneville, M., O'Brien, R.L., and Born, W.K. (2010). Gammadelta T cell effector functions: a blend of innate programming and acquired plasticity. Nat. Rev. Immunol. *10*, 467–478.

Cundy, K.C. (1999). Clinical pharmacokinetics of the antiviral nucleotide analogues cidofovir and adefovir. Clin. Pharmacokinet. *36*, 127–143.

De Clercq, E. (2004). Antiviral drugs in current clinical use. J. Clin. Virol. *30*, 115–133.

Delaglio, F., Grzesiek, S., Vuister, G.W., Zhu, G., Pfeifer, J., and Bax, A. (1995). NMRPipe: a multidimensional spectral processing system based on UNIX pipes. J. Biomol. NMR *6*, 277–293.

Fournié, J.J., Sicard, H., Poupot, M., Bezombes, C., Blanc, A., Romagné, F., Ysebaert, L., and Laurent, G. (2013). What lessons can be learned from γδ T cell-based cancer immunotherapy trials? Cell. Mol. Immunol. *10*, 35–41.

Gao, Y., Yang, W., Pan, M., Scully, E., Girardi, M., Augenlicht, L.H., Craft, J., and Yin, Z. (2003). Gamma delta T cells provide an early source of interferon gamma in tumor immunity. J. Exp. Med. *198*, 433–442.

Gomes, A.Q., Correia, D.V., Grosso, A.R., Lança, T., Ferreira, C., Lacerda, J.F., Barata, J.T., Silva, M.G., and Silva-Santos, B. (2010). Identification of a panel of ten cell surface protein antigens associated with immunotargeting of leukemias and lymphomas by peripheral blood gammadelta T cells. Haematologica *95*, 1397–1404.

Harly, C., Guillaume, Y., Nedellec, S., Peigné, C.M., Mönkkönen, H., Mönkkönen, J., Li, J., Kuball, J., Adams, E.J., Netzer, S., et al. (2012). Key implication of CD277/butyrophilin-3 (BTN3A) in cellular stress sensing by a major human γδ T-cell subset. Blood *120*, 2269–2279.

Hecker, S.J., and Erion, M.D. (2008). Prodrugs of phosphates and phosphonates. J. Med. Chem. *51*, 2328–2345.

Kim, M., Kleckley, T.S., Wiemer, A.J., Holstein, S.A., Hohl, R.J., and Wiemer, D.F. (2004). Synthesis and activity of fluorescent isoprenoid pyrophosphate analogues. J. Org. Chem. *69*, 8186–8193.

Kornberg, R.D., McNamee, M.G., and McConnell, H.M. (1972). Measurement of transmembrane potentials in phospholipid vesicles. Proc. Natl. Acad. Sci. USA *69*, 1508–1513.

Li, J., Cui, L., and He, W. (2005). Distinct pattern of human Vdelta1 gammadelta T cells recognizing MICA. Cell. Mol. Immunol. *2*, 253–258.

Li, H., Xiang, Z., Feng, T., Li, J., Liu, Y., Fan, Y., Lu, Q., Yin, Z., Yu, M., Shen, C., and Tu, W. (2013). Human Vγ9Vδ2-T cells efficiently kill influenza virus-infected lung alveolar epithelial cells. Cell. Mol. Immunol. *10*, 159–164.

Maalouf, M.A., Wiemer, A.J., Kuder, C.H., Hohl, R.J., and Wiemer, D.F. (2007). Synthesis of fluorescently tagged isoprenoid bisphosphonates that inhibit protein geranylgeranylation. Bioorg. Med. Chem. *15*, 1959–1966.

Marcellin, P., Chang, T.T., Lim, S.G., Tong, M.J., Sievert, W., Shiffman, M.L., Jeffers, L., Goodman, Z., Wulfsohn, M.S., et al.; Adefovir Dipivoxil 437 Study Group (2003). Adefovir dipivoxil for the treatment of hepatitis B e antigen-positive chronic hepatitis B. N. Engl. J. Med. *348*, 808–816.

McKenna, C., Higa, M., Cheung, N., and McKenna, M. (1977). Facile dealkylation of phosphonic acid dialkyl esters by Bromotrimethylsilane. Tetrahedron Lett. *18*, 155–158.

Miyagawa, F., Tanaka, Y., Yamashita, S., and Minato, N. (2001). Essential requirement of antigen presentation by monocyte lineage cells for the activation of primary human gamma delta T cells by aminobisphosphonate antigen. J. Immunol. *166*, 5508–5514.

Morita, C.T., Jin, C., Sarikonda, G., and Wang, H. (2007). Nonpeptide antigens, presentation mechanisms, and immunological memory of human Vgamma2Vdelta2 T cells: discriminating friend from foe through the recognition of prenyl pyrophosphate antigens. Immunol. Rev. *215*, 59–76.

Nussbaumer, O., Gruenbacher, G., Gander, H., Komuczki, J., Rahm, A., and Thurnher, M. (2013). Essential requirements of zoledronate-induced cytokine and γδ T cell proliferative responses. J. Immunol. *191*, 1346–1355.

Sandstrom, A., Peigné, C.M., Léger, A., Crooks, J.E., Konczak, F., Gesnel, M.C., Breathnach, R., Bonneville, M., Scotet, E., and Adams, E.J. (2014). The intracellular B30.2 domain of butyrophilin 3A1 binds phosphoantigens to mediate activation of human Vγ9Vδ2 T cells. Immunity *40*, 490–500.

Serafinowska, H.T., Ashton, R.J., Bailey, S., Harnden, M.R., Jackson, S.M., and Sutton, D. (1995). Synthesis and in vivo evaluation of prodrugs of 9-[2-(phosphonomethoxy)ethoxy]adenine. J. Med. Chem. *38*, 1372–1379.

Sicard, H., Ingoure, S., Luciani, B., Serraz, C., Fournié, J.J., Bonneville, M., Tiollier, J., and Romagné, F. (2005). In vivo immunomanipulation of V gamma 9V delta 2 T cells with a synthetic phosphoantigen in a preclinical nonhuman primate model. J. Immunol. *175*, 5471–5480.

Sireci, G., Espinosa, E., Di Sano, C., Dieli, F., Fournié, J.J., and Salerno, A. (2001). Differential activation of human gammadelta cells by nonpeptide phosphoantigens. Eur. J. Immunol. *31*, 1628–1635.

Thompson, K., and Rogers, M.J. (2004). Statins prevent bisphosphonate-induced gamma,delta-T-cell proliferation and activation in vitro. J. Bone Miner. Res. *19*, 278–288.

Van Beek, E.R., Löwik, C.W., and Papapoulos, S.E. (2002). Bisphosphonates suppress bone resorption by a direct effect on early osteoclast precursors without affecting the osteoclastogenic capacity of osteogenic cells: the role of protein geranylgeranylation in the action of nitrogen-containing bisphosphonates on osteoclast precursors. Bone *30*, 64–70.

Vavassori, S., Kumar, A., Wan, G.S., Ramanjaneyulu, G.S., Cavallari, M., El Daker, S., Beddoe, T., Theodossis, A., Williams, N.K., Gostick, E., et al. (2013). Butyrophilin 3A1 binds phosphorylated antigens and stimulates human γδ T cells. Nat. Immunol. *14*, 908–916.

Vranken, W.F., Boucher, W., Stevens, T.J., Fogh, R.H., Pajon, A., Llinas, M., Ulrich, E.L., Markley, J.L., Ionides, J., and Laue, E.D. (2005). The CCPN data model for NMR spectroscopy: development of a software pipeline. Proteins *59*, 687–696.

Wang, T., Gao, Y., Scully, E., Davis, C.T., Anderson, J.F., Welte, T., Ledizet, M., Koski, R., Madri, J.A., Barrett, A., et al. (2006). Gamma delta T cells facilitate adaptive immunity against West Nile virus infection in mice. J. Immunol. *177*, 1825–1832.

Wang, H., Henry, O., Distefano, M.D., Wang, Y.C., Räikkönen, J., Mönkkönen, J., Tanaka, Y., and Morita, C.T. (2013). Butyrophilin 3A1 plays an essential role in prenyl pyrophosphate stimulation of human Vγ2Vδ2 T cells. J. Immunol. *191*, 1029–1042.

Wiemer, A.J., Yu, J.S., Shull, L.W., Barney, R.J., Wasko, B.M., Lamb, K.M., Hohl, R.J., and Wiemer, D.F. (2008). Pivaloyloxymethyl-modified isoprenoid bisphosphonates display enhanced inhibition of cellular geranylgeranylation. Bioorg. Med. Chem. *16*, 3652–3660.

Wiemer, A.J., Wernimont, S.A., Cung, T.D., Bennin, D.A., Beggs, H.E., and Huttenlocher, A. (2013). The focal adhesion kinase inhibitor PF-562,271 impairs primary CD4+ T cell activation. Biochem. Pharmacol. *86*, 770–781.

Wiemer, D.F., and Wiemer, A.J. (2014). Opportunities and challenges in development of phosphoantigens as Vγ9Vδ2 T cell agonists. Biochem. Pharmacol. *89*, 301–312.

Wrobel, P., Shojaei, H., Schittek, B., Gieseler, F., Wollenberg, B., Kalthoff, H., Kabelitz, D., and Wesch, D. (2007). Lysis of a broad range of epithelial tumor cells by human gamma delta T cells: involvement of NKG2D ligands and T-cell receptor- versus NKG2D-dependent recognition. Scand. J. Immunol. *66*, 320–328.